Identification of cytoplasmic residues of Sec61p involved in ribosome binding and cotranslational translocation

Zhiliang Cheng, Ying Jiang, Elisabet C. Mandon, and Reid Gilmore

Department of Biochemistry and Molecular Pharmacology, University of Massachusetts Medical School, Worcester, MA 01605

The cytoplasmic surface of Sec61p is the binding site for the ribosome and has been proposed to interact with the signal recognition particle receptor during targeting of the ribosome nascent chain complex to the translocation channel. Point mutations in cytoplasmic loops six (L6) and eight (L8) of yeast Sec61p cause reductions in growth rates and defects in the translocation of nascent polypeptides that use the cotranslational translocation pathway. Sec61 heterotrimers isolated from the L8 *sec61* mutants have a greatly reduced affinity for 80S ribosomes. Cytoplasmic accumulation of protein precursors demonstrates that the initial contact between the large ribosomal subunit and the Sec61 complex is important for efficient insertion of a nascent polypeptide into the translocation pore. In contrast, point mutations in L6 of Sec61p inhibit cotranslational translocation without significantly reducing the ribosome-binding activity, indicating that the L6 and L8 *sec61* mutants affect different steps in the cotranslational translocation pathway.

Introduction

Translocation of proteins across the RER can occur by cotranslational or posttranslational pathways. The signal sequence of a protein that is translocated by the cotranslational pathway is recognized by the signal recognition particle (SRP) as the nascent chain emerges from the polypeptide exit site on the large ribosomal subunit (Walter and Johnson, 1994; Halic et al., 2004). Targeting to the RER is mediated by the interaction between the SRP–ribosome nascent chain (RNC) complex and the SRP receptor (SR; Mandon et al., 2003), which initiates a GTPase cycle that culminates in attachment of the RNC to the protein translocation channel (Song et al., 2000). In *Saccharomyces cerevisiae*, proteins that are translocated by the posttranslational pathway are not targeted to the Sec61 translocation channel by SRP, but are instead delivered to the Sec complex by cytosolic Hsp70 proteins (for review see Corsi and Schekman, 1996). Translocons that mediate cotranslational translocation are oligomers formed from three to four copies of a Sec61 heterotrimer (Beckmann et al., 2001; Morgan et al., 2002) that is in turn composed of Sec61p, Sbh1p, and Sss1p (Panzner et al., 1995). The Sec complex is composed of a Sec61 translocon plus the Sec62–Sec63 complex (Deshaies et al., 1991; Panzner et al., 1995). Yeast Ssh1p, a distantly related homologue of Sec61p, assembles with Sbh2p and Sss1p to form an auxiliary translocon that is specific for the cotranslational pathway (Finke et al., 1996; Wittke et al., 2002). Ssh1p translocons are not incorporated into the Sec complex (Finke et al., 1996), hence, overexpression of Ssh1p cannot compensate for loss of Sec61p.

The relative contributions of the co- and posttranslational pathways to precursor transport across the RER have been extensively investigated in *S. cerevisiae*. Partitioning of nascent polypeptides between the targeting pathways is governed by the relative hydrophobicity of the signal sequence (Ng et al., 1996), with SRP selecting more hydrophobic signals for the cotranslational pathway. Although the cotranslational pathway is the predominant pathway in vertebrate organisms, SRP and the SR are dispensable in *S. cerevisiae* (Hann and Walter, 1991; Ogg et al., 1992).

The predicted topology of yeast Sec61p in the ER (Wilkinson et al., 1996) has now been refined by the structural determination of the archaebacterial translocation channel SecYEG (Van den Berg et al., 2004). The NH_2 and COOH termini of Sec61p and the even-numbered loops (L2, L4, L6, and L8) that separate the 10 membrane spans face the cytoplasm. Proteolytic mapping experiments of canine Sec61α indicated

Z. Cheng and Y. Jiang contributed equally to this paper.

Correspondence to Reid Gilmore: reid.gilmore@umassmed.edu

Abbreviations used in this paper: CPY, carboxypeptidase Y; DPAPB, dipeptidylaminopeptidase B; DPAPB-HA, HA-tagged DPAPB; Endo H, endoglycosidase H; PK-RM, puromycin-high salt-washed rough microsomes; RNC, ribosome nascent chain; SR, SRP receptor; SRP, signal recognition particle.

The Journal of Cell Biology, Vol. 168, No. 1, January 3, 2005 67–77
http://www.jcb.org/cgi/doi/10.1083/jcb.200408188

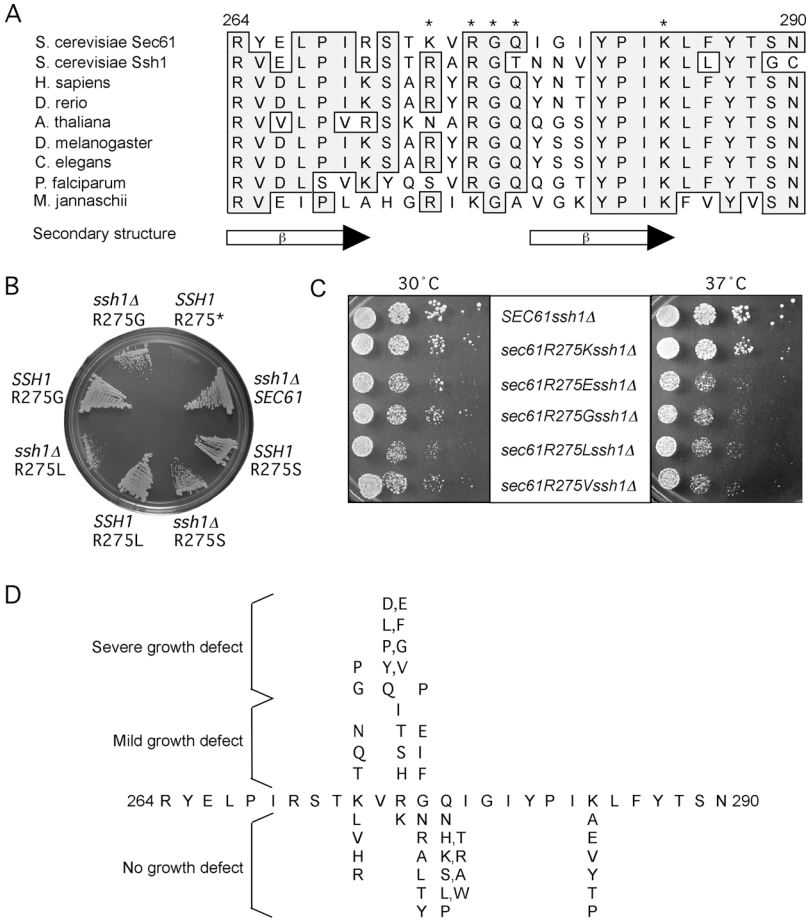

Figure 1. **Point mutations in L6 of Sec61p.** (A) Secondary structure of L6 (*M. jannaschii* SecY) and sequence alignment between eukaryotic and *M. jannaschii* L6 segments. Identities are boxed and asterisks indicate residues subjected to mutagenesis. (B) Yeast strains RGY401 (*ssh1Δ*) and RGY402 (*SSH1*) that had been transformed with plasmids expressing wild-type or mutant (R275*, R275S, R275L, or R275G) alleles of Sec61p were streaked on 5-fluoroorotic acid plates and allowed to grow for 2 d at 30°C. Sec61R275* has a termination codon at position 275. (C and D) Growth rates of L6 *sec61* mutants were compared by serial dilution analysis (C) as described in Materials and methods and used to assign the L6 *sec61ssh1Δ* mutants to growth phenotype categories (D).

that L6 and L8 are highly exposed on the cytoplasmic surface of the Sec61 complex (Song et al., 2000). Proteolysis of canine Sec61α in L6 and L8 inhibits SRP-dependent translocation activity (Song et al., 2000) and eliminates ribosome binding to the translocon (Raden et al., 2000). Nonetheless, the detailed mechanism that allows transfer of the RNC from the GTP-bound conformation of the SRP–SR complex to the translocon is poorly understood. The ribosome-binding site on the translocation channel has not been mapped with precision. Because L6 and L8 have a net positive charge, it was not clear whether specific residues, rather than the overall charge distribution, were important for the ribosome-binding affinity of the Sec61 complex. Here, we have identified residues in L6 and L8 of Sec61p that are critical for the cotranslational translocation pathway, and defined segments of Sec61p that interact with the ribosome and possibly with the SR.

Results

Mutagenesis of cytosolic loops of Sec61p

A sequence comparison of L6 of Sec61 from diverse eukaryotes reveals a high degree of amino acid identity, particularly in the segments that are proximal to transmembrane spans 6 and 7 (Fig. 1 A). A seven-residue loop, which connects two β strands in the *Methanococcus jannaschii* SecY structure (Van den Berg et al., 2004), contains several highly conserved polar residues (K273, R275, and Q277). These three residues, together with G276 and K284, were selected for site-directed mutagenesis in *S. cerevisiae* Sec61p. The haploid BWY12 was chosen as a starting strain to analyze yeast *sec61* mutants using a plasmid shuffle procedure. In BWY12, a *HIS3*-marked disruption of the essential *SEC61* gene is rescued by the *URA3*-marked CEN plasmid pBW7 that encodes Sec61p. We disrupted the nonessential *SSH1* gene to provide a sensitized genetic background for the analysis of the Sec61p mutants. Although the initial description of an *ssh1Δ* strain noted a minor decrease in growth rate (Finke et al., 1996), a more recent paper reported that a yeast strain lacking Ssh1p rapidly acquires a petite phenotype when grown on a fermentable carbon source and displays severe defects in protein translocation and dislocation when maintained on a nonfermentable carbon source (Wilkinson et al., 2001). As shown in Fig. 3 A, the growth phenotype of our *ssh1Δ* strain (RGY401) was consistent with the initial report (Finke et al., 1996), hence, this strain was suitable for the analysis of L6 and L8 *sec61* mutants. For example, when RGY401 cells are grown on glucose-containing media (YPD or synthetic defined [SD]), petite (ρ^-) cells arise at a low frequency (~0.3%/cell division).

RGY401 (*ssh1Δ*) and RGY402 (*SSH1*) were transformed with *LEU2*-marked plasmids encoding *sec61* point mutants and plated on media containing 5-fluoroorotic acid to select against

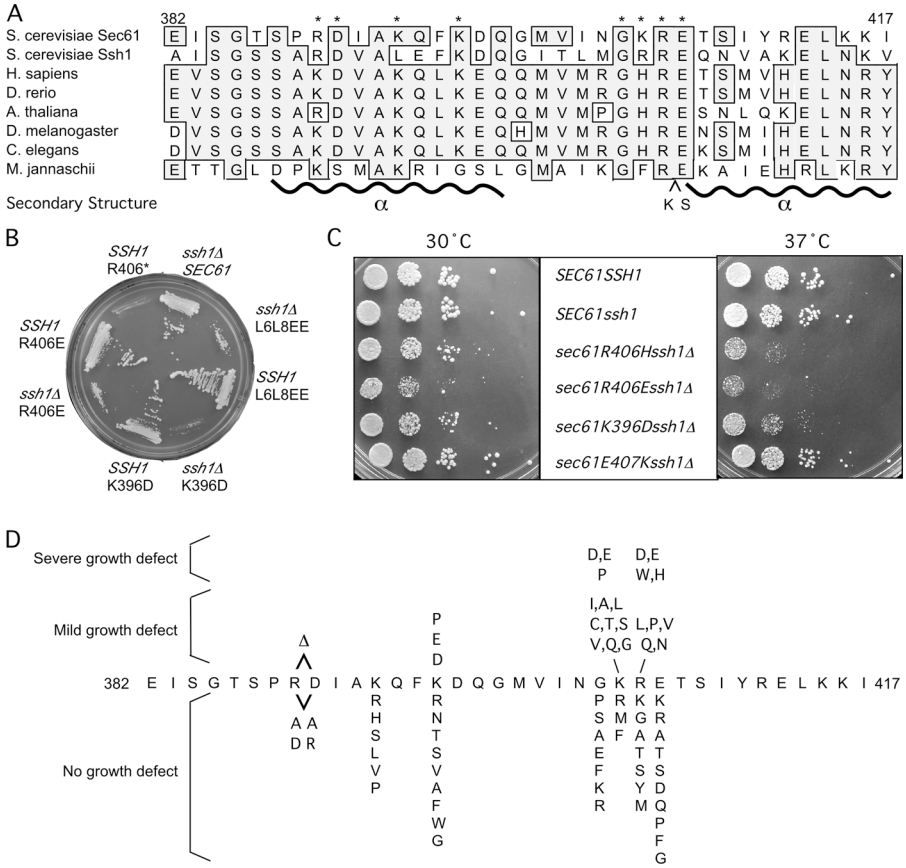

Figure 2. **Point mutations in L8 of Sec61p.** (A) Secondary structure of L8 (*M. jannaschii* SecY) and sequence alignment between eukaryotic and *M. jannaschii* L8 segments. The locations of α-helical segments in L8 of *M. jannaschii* SecY are indicated below the alignment. Identities are boxed and asterisks indicate residues subjected to mutagenesis. The L8 region of *M. jannaschii* SecY contains a two-residue insertion (KS) relative to eukaryotic Sec61 sequences. (B) Yeast strains RGY401 (*ssh1Δ*) and RGY402 (*SSH1*) that had been transformed with plasmids expressing wild-type *SEC61*, or mutant alleles (R406*, R406E, L6L8EE, or K396D) of Sec61p were streaked onto 5-fluoroorotic acid plates and allowed to grow for 2 d at 30°C. (C and D) Serial dilution experiments were performed as described in Fig. 1 C's legend and used to assign the L8 *sec61ssh1Δ* mutants to growth phenotype categories (D).

retention of pBW7 (Fig. 1 B). Positive and negative controls for the screen are based on the observations that Ssh1p is nonessential (*SEC61ssh1Δ* is viable) and that expression of Ssh1p cannot suppress a *sec61*-null mutant (*sec61R275*SSH1* is not viable). Amino acid substitutions at R275 cause a growth rate defect in the absence, but not in the presence, of Ssh1p. Differences in growth rate were evaluated by plating serial dilutions of cells onto YPD (Fig. 1 C) or YPEG plates. With the exception of lysine (*sec61R275Kssh1Δ*), amino acid substitutions at R275 cause obvious reductions in growth rate at 30°C that are accentuated at 37°C and not apparent at 18°C (not depicted). Reductions in the growth rates of the mutants relative to RGY401 or RGY402 were slightly less obvious on YPEG plates (unpublished data). The effects of L6 point mutations are summarized in Fig. 1 D. Substitutions that reverse the charge (R275D or R275E) or substitute an aliphatic or aromatic amino acid for arginine cause a severe growth defect. Less severe growth defects were caused by substitutions of polar (R275S or R275T) or positively charged amino acids (e.g., R275H). A wider variety of substitutions were tolerated at K273 and G276. The triple charge–reversal mutant (*sec61K273D*, *R275D*, and *K284Dssh1Δ*) designated *sec61L6DDD* has a more severe growth defect than *sec61R275Dssh1Δ* (not depicted).

Several conserved residues between R389 and E407 were selected for mutagenesis based on a sequence comparison of the L8 region of eukaryotic Sec61 (Fig. 2 A). The structure of *M. jannaschii* SecY indicates that four of these residues (G404, K405, R406, and E407) are located in the tip of the L8 loop between two α helices that project into the cytoplasm from the membrane surface. Point mutations in L8 did not cause a growth rate defect in strains that express Ssh1p (Fig. 2 B). Serial dilution experiments (Fig. 2 C) demonstrated that mutations at K405, R406, and, to a lesser extent, K396 cause growth rate defects (Fig. 2 D). Substitutions at the other tested residues had little or no effect, including a two-residue deletion (R389ΔD390Δ). A double mutant (L6L8EE) that combined two severe L6 and L8 mutations (*R275E* and *R406E*) was suppressed by expression of Ssh1p (Fig. 2 B).

Decreased growth rates correlate with protein translocation defects

RGY401 derivatives expressing L6 or L8 *sec61* mutants lose respiratory competence at a 3–10-fold higher frequency (~1–3% per generation) than the parental *ssh1Δ* strain. RGY401 and its derivatives were maintained on SEG media (synthetic minimal media containing 2% ethanol and 3% glycerol) to select against the accumulation of ρ^- cells. When growth rates were determined after shifting cells into YPD media, the *ssh1Δ* mutant showed a 10–20% decrease in growth rate relative to the wild-type strain (Fig. 3 A), a result that is consistent with the initial description of an *ssh1Δ* mutant (Finke et al., 1996). The *sec61R275E* and *sec61R406E ssh1Δ* strains showed a 2.5-fold decrease in growth rate at 30°C, relative to the parental *ssh1Δ* strain (Fig. 3 A).

The *sec61* L6 and L8 mutants were tested for defects in the translocation of the SRP-dependent substrate dipepti-

dylaminopeptidase B (DPAPB) and the SRP-independent substrate carboxypeptidase Y (CPY). To facilitate detection of DPAPB, selected RGY401 derivatives were transformed with a low copy plasmid that encodes HA-tagged DPAPB (DPAPB-HA; Ng et al., 1996). Wild-type and mutant cultures were pulse labeled with ^{35}S-amino acids 4 h after cells were shifted into SD media (Fig. 3 B). Integration of the type II membrane protein DPAPB into the RER is accompanied by the addition of seven to eight N-linked oligosaccharides. Unglycosylated DPAPB-HA synthesized by tunicamycin-treated cells (Fig. 3 B, wt +TM) served as a mobility marker for the nontranslocated precursor (p-DPAPB-HA). The pulse-labeling experiments revealed a reduction in DPAPB translocation in the *ssh1Δ* mutant (Fig. 3 B) that was greatest 4 h after transfer into SD media (Fig. 3 C). Importantly, the percentage of nontranslocated DPAPB (15–20% at 4 h) was fourfold lower than previously reported for an *ssh1Δ* strain (Wilkinson et al., 2001). A more significant defect in DPAPB translocation was detected in L8 *sec61ssh1Δ* strains (Fig. 3 B). Expression of Ssh1p suppressed the translocation defect caused by point mutations in L8, which is consistent with the lack of a growth defect. Although DPAPB integration in wild-type cells was efficient at all time points after the shift to SD media (Fig. 3 C, closed squares), transport defects for the L6 (triangles) and L8 (open squares) *sec61ssh1Δ* mutants reached a peak 4 h after cells were transferred into the SD media, and declined thereafter.

Nonglycosylated CPY obtained by labeling cells in the presence of tunicamycin was used as a mobility marker for prepro-CPY (Fig. 3 D). As expected, there was little or no production of the Golgi (Fig. 3 D, p2) or of mature vacuolar forms of CPY during the 7-min pulse-labeling period. Translocation of CPY was similar in the wild-type and *ssh1Δ* strains, which is consistent with the observation that the Ssh1p heterotrimer is not incorporated into the Sec complex. Although point mutations in L8 do not cause a translocation defect when expressed in an *SSH1* strain, there was a substantial reduction in CPY translocation when the *sec61* mutants were tested in the *ssh1Δ* strain. Endoglycosidase H (Endo H) digestion experiments confirmed that the protein designated as ppCPY was the precursor, and not comigrating mature CPY (unpublished data). Conceivably, a defect in N-linked glycosylation could cause the accumulation of nonglycosylated p1CPY. To test this possibility, we pulse labeled spheroplasts prepared from the *sec61L6DDD* mutant for 7 min, and then performed osmotic lysis. As shown in Fig. 3 E, the majority of p1CPY was trypsin resistant in the absence of detergent, unlike ppCPY, which was accessible to the protease. As observed for DPAPB integration (Fig. 3 C), the maximal defect in CPY translocation was observed 4 h after transfer of cells into SD media (not depicted). Suppression of a CPY transport defect in the *SSH1* strain is unlikely to occur by transport of CPY through an Ssh1p translocon (Wittke et al., 2002), which suggests that reduced translocation of CPY in the L8 *sec61* mutants arises by an indirect mechanism.

A larger collection of the L6 and L8 *sec61* mutants were assayed for defects in the translocation of DPAPB-HA, CPY, and a second SRP-independent substrate (Gas1p; Fig. 4). Between 30 and 50% of the DPAPB was not integrated in each of

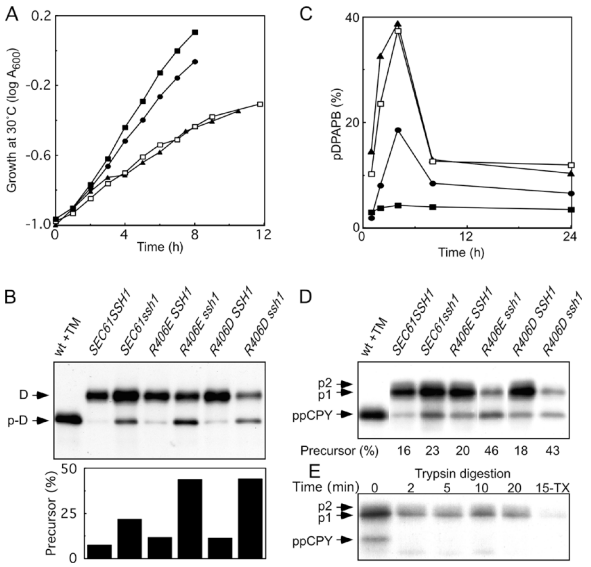

Figure 3. **Translocation defects in *sec61* mutants are suppressed by expression of Ssh1p.** (A) Wild-type yeast (RGY402; closed squares) and *ssh1Δ* mutants expressing wild-type Sec61p (circles), *sec61R275E* (open squares), or *sec61R406E* (triangles) were grown to mid-log phase at 30°C in SEG media. The cultures were diluted into YPD media at 0 h and allowed to grow for 8–12 h at 30°C. (B and D) Wild-type and mutant yeast cultures were pulse labeled for 7 min at 30°C after 4 h of growth in SD media at 30°C. One sample of wild-type cells was treated with tunicamycin (wt + TM) for 30 min before pulse labeling. DPAPB-HA (B) and CPY (D) immunoprecipitates were resolved by SDS-PAGE. The ER (p1), Golgi (p2), and precursor (ppCPY) forms of CPY and the glycosylated (D) and nonglycosylated (p-D) forms of DPAPB-HA are labeled. In D, white lines indicate that intervening lanes of Endo H digestion products have been removed for clarity. Translocation of CPY or integration of DPAPB-HA was quantified with a BioRad FX Molecular Imager. (C) Wild-type yeast (RGY402; closed squares) and *ssh1Δ* mutants expressing wild-type Sec61p (circles), *sec61R275E* (triangles), or *sec61R406E* (open squares) were pulse labeled to evaluate integration of DPAPB-HA as described in B, after 1, 2, 4, 8, or 24 h of growth in SD media. As needed, cell cultures were diluted with fresh SD media to maintain an A_{600} of <0.8. (E) Pulse-labeled *sec61L6DDD* spheroplasts were osmotically lysed and centrifuged at 500 *g* to remove unbroken cells. Spheroplast lysates were incubated on ice with trypsin (100 μg/ml) as indicated. The lane designated 15-TX contained trypsin plus Triton X-100. Trypsin was inactivated with PMSF before immunoprecipitation.

the *sec61ssh1Δ* mutants that were tested. Deficiencies in CPY translocation showed significantly greater variation, with some substitutions (e.g., R275F and R275V) causing only minor defects relative to the parental *ssh1Δ* strain. Gas1p was analyzed to determine whether the L6 and L8 *sec61* mutants have defects in the translocation of other substrates that use the post-translational translocation pathway. The percentage of Gas1p that was not translocated during the 7-min pulse was much lower than observed for CPY. Together with the genetic evidence presented in Figs. 1–3, these data suggest that mutations in L6 and L8 preferentially interfere with the SRP-dependent translocation pathway.

Impact of *sec61* mutations on protein dislocation and precursor accumulation

A mutation that reduces folding of Sec61p should inhibit all protein transport pathways that are mediated by the translocon, because of a reduction in the cellular content of the Sec61 het-

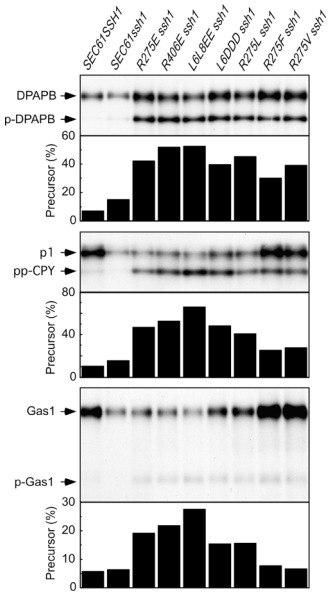

Figure 4. **Differential effect of Sec61p mutations on SRP-dependent and SRP-independent translocation pathways.** Integration of DPAPB-HA and translocation of CPY and Gas1p were evaluated by pulse labeling of wild-type and mutant yeast strains that were grown for 4 h in SD media at 30°C. Pulse labeling and immunoprecipitation of proteins were conducted as described in Fig. 3's legend.

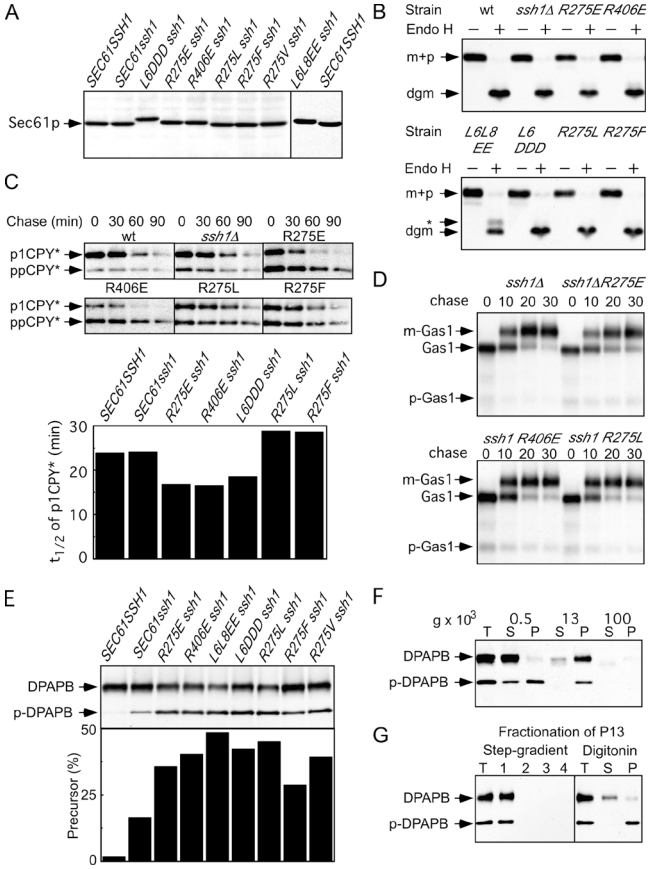

Figure 5. **Transport pathways affected by Sec61 mutations.** All experiments were conducted after 4 h of growth in SD media at 30°C. (A) Equal amounts of total protein (25 μg) were resolved by SDS-PAGE for protein immunoblot analysis using a COOH-terminal–specific antibody to Sec61p. (B) Total cell extracts were prepared for SDS-PAGE with or without prior digestion by Endo H. Deglycosylated mature CPY (dgm) is resolved from vacuolar CPY (m) and nontranslocated prepro-CPY (p). The asterisk designates an incomplete Endo H digestion product. (C) Degradation of CPY^*_{HA} in L6 and L8 *sec61* mutants. Cell extracts prepared at 30-min intervals after cycloheximide addition were resolved by SDS-PAGE. Nontranslocated $ppCPY^*_{HA}$ and translocated $p1CPY^*_{HA}$ were detected using anti-HA antibodies. Protease digestion experiments confirmed that $p1CPY^*_{HA}$, but not $ppCPY^*_{HA}$, was in a membrane-enclosed compartment (not depicted). The apparent half-life of $p1CPY^*_{HA}$, determined according to a first-order decay process, is plotted below representative time courses. (D) Yeast cultures were pulse labeled for 7 min and chased for 10, 20, or 30 min. The nontranslocated precursor (p-Gas1), the translocated ER form (Gas1), and the mature form (m-Gas1) of Gas1p are labeled. (E) Protein immunoblot detection of p-DPAPB-HA and mature DPAPB-HA in total cell extracts resolved by SDS-PAGE. Protein immunoblots (C and E) were quantified by densitometry. (F) Differential centrifugation of spheroplast lysates prepared from the *sec61L6DDDssh1Δ* mutant. Total lysates (T) and supernatant (S) and pellet (P) fractions were obtained after centrifugation at 500 *g*, 13,000 *g*, and 100,000 *g*. (G) The P13 fraction (T) was resuspended in buffer A (50 mM Hepes, pH 7.5, 150 mM KOAc, 5 mM $Mg(OAc)_2$, and 1 mM DTT) adjusted to 250 mM sucrose and applied to a sucrose step gradient in buffer A with 1.6-M and 2-M sucrose layers. After centrifugation for 1 h at 100,000 *g*, the gradient was resolved into the following fractions: (1) 0.25 sample load plus 0.25/1.6-M interface, (2) 1.6-M sucrose layer plus 1.6/2-M interface, (3) 2-M sucrose layer, and (4) pellet. The P13 fraction (T) was solubilized in 3% digitonin and 500 mM KOAc and centrifuged at 100,000 *g* for 1 h to obtain supernatant (S) and pellet (P) fractions.

erotrimer. Identical amounts of total protein extracts of yeast cells were resolved by SDS-PAGE for a subsequent protein immunoblot using antibodies specific for Sec61p (Fig. 5 A). Similar amounts of Sec61p were expressed in the wild type and in the L6 and L8 *sec61* mutants. Migration differences between lanes are explained by increases in the number of acidic residues in the mutant proteins. Thus, the translocation defects are not explained by a reduction in the cellular content of Sec61p.

Cytoplasmic precursors (preKar2p, prepro-CPY, and prepro–α factor) that are translocated through the Sec complex are readily detected by protein immunoblot analysis when *sec62* or *lhs1* mutants are analyzed at a semipermissive temperature (Baxter et al., 1996; Hamilton and Flynn, 1996). Protein immunoblot analysis of total cell extracts prepared from the L6 and L8 *sec61* mutants revealed a single immunoreactive species for CPY (Fig. 5 B). Mature CPY comigrates with prepro-CPY because of cleavage of the propeptide in the vacuole. Deglycosylation of mature CPY with Endo H resolved prepro-CPY from deglycosylated mature CPY. Prepro-CPY was only faintly visible in the Endo H–digested lanes, which demonstrates that the majority of the CPY precursor detected in a 7-min pulse-labeling experiment is subsequently translocated into the ER.

Additional evidence supporting a minor kinetic delay in transport of SRP-independent precursors was obtained by pulse-chase analysis of Gas1p biosynthesis (Fig. 5 D). Although the Gas1p precursor was detected after the 7-min pulse, the majority of the precursor was translocated into the ER during the subsequent 10-min chase (Fig. 5 D). These results suggest that there is a reduction in transport rate for precursors that use the Sec complex.

Dislocation of unfolded proteins from the ER lumen back into the cytosol for degradation by the proteasome is thought to occur through the Sec61 complex (Wiertz et al., 1996). Degradation of the well characterized degradation substrate CPY^*_{HA} was monitored using a cycloheximide-chase procedure (Spear

and Ng, 2003), as the apparent rate of dislocation determined by this method should not be perturbed by the kinetic delay in CPY*$_{HA}$ translocation (Fig. 5 C). The p1 form of CPY*$_{HA}$ was degraded rapidly, with a calculated half life of <30 min in all strains (Fig. 5 C), suggesting that mutations in L6 and L8 of Sec61p do not interfere with the dislocation pathway. Mutations in gene products that are required for CPY*$_{HA}$ dislocation typically increase the half-life of degradation to ~1 h (Spear and Ng, 2003).

Protein immunoblots showed that the nontranslocated DPAPB-HA precursor accumulates in the *sec61* mutants after 4 h of growth in SD media (Fig. 5 E). Cellular accumulation of pDPAPB-HA was elevated two to threefold, relative to the *ssh1Δ* mutant, and reached a maximal value 6–8 h after the *sec61* mutants were transferred into SD media (unpublished data). We next asked whether the nontranslocated DPAPB was soluble or membrane associated. Differential centrifugation of spheroplast lysates achieved a partial resolution of the pDPAPB-HA from DPAPB-HA (Fig. 5 F). As expected, DPAPB-HA was recovered in the P13 fraction that contains vacuoles. RER membranes, as detected using antibodies to the oligosaccharyltransferase subunit Ost1p, were enriched in the P0.5 and P13 fractions (not depicted). The precursor (pDPAPB-HA) was not in the cytosol fraction (S100), but instead sedimented at low and intermediate speeds. Subsequent centrifugation of the P13 fraction on a sucrose step gradient demonstrated that the precursor was membrane associated, because it did not sediment through a 1.6-M sucrose cushion (Fig. 5 G). In contrast to mature DPAPB-HA, the precursor was insoluble in the nonionic detergent digitonin (Fig. 5 G), which suggests that it is incorporated into a membrane-associated aggregate. These results suggest that pDPAPB-HA molecules that are not translocated by the SRP-dependent pathway rapidly adopt a translocation-incompetent conformation.

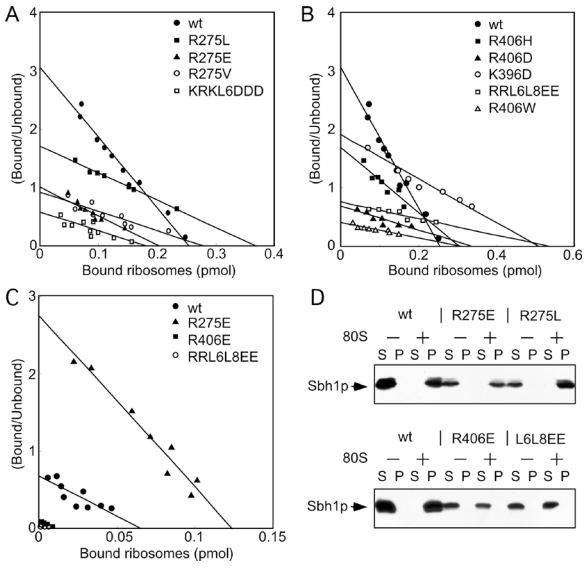

Figure 6. **Binding of ribosomes to yeast PK-RM and Sec61 proteoliposomes.** (A–C) Scatchard plots of ribosome binding to PK-RM (A and B) or Sec61p proteoliposomes (C) isolated from wild type (*SEC61ssh1Δ*) or from L6 (A and C) and L8 (B and C) *sec61ssh1Δ* mutants. (D) Sec61 heterotrimers (150–300 fmol) purified from wild type and from selected L6 and L8 mutants were incubated in the presence or absence of 900 fmol of yeast ribosomes before centrifugation to obtain supernatant (S) and pellet (P) fractions. After SDS-PAGE, Sbh1p was detected using anti-FLAG antibodies.

Defects in ribosome binding

Microsomal membranes that were isolated from the *ssh1Δ* strain, as well as several L6 and L8 *sec61ssh1*Δ mutants, were treated with puromycin and high salt to remove endogenous membrane-bound ribosomes. The resulting ribosome-stripped microsomes (puromycin-high salt-washed rough microsomes; PK-RM) were assayed for ribosome-binding activity in a physiological ionic strength buffer (Fig. 6, A and B). PK-RM prepared from the *ssh1Δ* strain bind ribosomes in a saturable manner (Fig. 6 A, closed circles), with a binding affinity (K_d = 5.5 ± 0.5 nM) that is in good agreement with previous reports (Prinz et al., 2000a,b). The negative reciprocal of the slope of a Scatchard plot is proportional to the K_d, so a decrease in slope corresponds to a decrease in binding affinity. Mutagenesis of R275 to aliphatic or acidic residues (Fig. 6 A) caused a minor reduction in apparent ribosome-binding affinity (R275L, K_d = 13.1 ± 0.3 nM; R275E, K_d = 15.7 ± 3.2 nM; and R275V, K_d = 20.7 ± 3.5 nM). The ribosome-binding affinity of the triple mutant (L6DDD) was similar (K_d = 17 ± 2.6 nM), which suggests that basic residues in L6 are not the primary determinants for the ribosome–Sec61p interaction. Point mutations in L8 (Fig. 6 B) that caused mild growth defects also reduced the ribosome-binding affinity by two to threefold (K396D, K_d = 18.2 ± 1.7 nM; and R406H, K_d = 11.3 ± 1.5 nM). Less conservative substitutions at R406 caused a more significant decrease in ribosome-binding affinity (R406D, K_d = 37.4 ± 10.6 nM; R406W, K_d = 54.2 ± 9.8 nM; and RRL6L8EE, K_d = 38.2 ± 7.7 nM).

The reduction in ribosome-binding affinity caused by several L8 *sec61* mutations was accompanied by an apparent increase in ribosome binding sites, suggesting that the residual binding activity might be nonspecific. To test this possibility, we purified wild-type and mutant Sec61 heterotrimers from yeast strains expressing an affinity-tagged derivative (His_6-FLAG-Sbh1p) of the Sbh1p subunit of the Sec61 complex. The ribosome-binding affinity of purified Sec61 translocons was determined after reconstitution into liposomes (Fig. 6 C). Proteoliposomes prepared with wild-type Sec61p and an L6 mutant had similar binding affinities for the 80S ribosome (wild type, K_d = 6.5 ± 1.7 nM; R275E, K_d = 2.3 ± 0.4 nM). In contrast, proteoliposomes prepared with *sec61* R406E or *sec61* L6L8EE had a dramatically reduced capacity and affinity for the ribosome (Fig. 6 C), even though they contained comparable amounts of Sec61p (not depicted). The Sec61p–ribosome interaction was also monitored in detergent solution using a cosedimentation assay (Prinz et al., 2000a). Wild-type and mutant Sec61p heterotrimers, as detected using anti-FLAG sera (Fig. 6 D) or antibody to Sec61p (not depicted), were recovered in the supernatant fraction, in the absence of added ribosomes. Purified wild-type Sec61p heterotrimers and two different L6 mutants (R275E and R275L) quantitatively cosedimented with ribosomes in this assay (Fig. 6 D). Cosedimentation of the L8 mutant (R406E) and the L6L8 double mutant (RRL6L8EE)

with the ribosome was undetectable using anti-FLAG sera (Fig. 6 D) or antibody to Sec61p (not depicted). The identity of the protein or proteins responsible for the residual ribosome-binding activity of PK-RM isolated from the L8 mutants is unknown.

Discussion

Isolation of a novel class of *sec61* mutants

Alleles of *sec61* that selectively interfere with the cotranslational translocation pathway have not been described previously, in part because expression of Ssh1p suppresses the related growth and translocation defects. Two temperature-sensitive *sec61* alleles (*sec61-2* and *sec61-3*) encode unstable proteins that are degraded at the restrictive temperature (Sommer and Jentsch, 1993), and hence do not display selective defects in translocation or dislocation at the restrictive temperature (Stirling et al., 1992; Plemper et al., 1997). A screen for cold-sensitive *sec61* mutants yielded several strains (*sec61-8*, *sec61-10*, and *sec61-110*) that were primarily defective in the transport of substrates that use the posttranslational translocation pathway (Pilon et al., 1998).

Cytosolic loops of Sec61p are critical for cotranslational translocation

Mutagenesis of yeast Sec61p can be interpreted in the context of the recently solved X-ray structure of *M. jannaschii* SecYEG, because the lengths and, to a lesser extent, the sequences of L6 and L8 are well conserved between the archae and eukaryotic translocation channels. The amphipathic H_2 α helix in SecE (γ-subunit, homologous to Sss1p) defines the interface between the membrane and the cytosol (Van den Berg et al., 2004). L6 and L8 of SecY project ~20 Å into the cytosol from the membrane surface (Fig. 7 A). Four (K273, R275, G276, and Q277) of the five residues in L6 that were selected for mutagenesis are located at the tip of the loop between two β strands, whereas the fifth residue (K284) is located near the polar head group region of the membrane bilayer (Fig. 7 B). Examination of the corresponding residues (R239 and K241) in *M. jannaschii* SecYEG reveals that the positively charged side chains of K273 and R275 are exposed and oriented toward the cytosol. In contrast, the side chain on A243 (Q277 in Sec61p) is oriented toward the membrane surface, which likely explains why point mutations at this site do not cause growth defects. Point mutations at G276 (G242 in *M. jannaschii*) that cause growth defects in *S. cerevisiae* might do so by introducing a negative charge (G275E) or by reducing the flexibility of L6 (e.g., G276P).

Four of the eight residues selected for mutagenesis in L8 of Sec61 are located in the tip of a loop that connects two α-helical segments (Fig. 7 B). The importance of K405 and R406 in Sec61p is readily explained by the orientation and location of the corresponding side chains (F359 and K360) in *M. jannaschii* SecY (Fig. 7 B). Interestingly, replacement of K405 with phenylalanine (as in *M. jannaschii* SecY) did not cause growth or translocation defects (unpublished data), which indicates

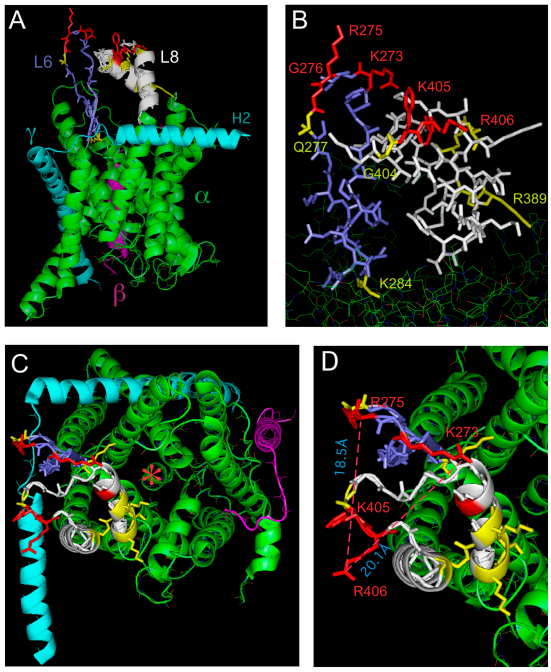

Figure 7. **Point mutations in L6 and L8 define a contact surface for cytoplasmic ligands of the Sec61 complex.** (A) A ribbon diagram of SecYEG complex showing the three subunits (SecY, green; SecE, cyan; and SecG, magenta) as viewed from within the plane of the membrane. The L6 (blue) and L8 (white) regions in SecY are highlighted. The SecY residue that aligns with a Sec61 residue subjected to mutagenesis is designated by a colored side chain; mutagenesis of red, but not yellow, side chains caused growth defects. (B) An expanded view of A showing that the critical residues in Sec61p are located at the tips of L6 and L8. (C) A top view of the SecYEG complex. The subunits, loops, and mutagenized residues are colored as in A. The dimerization interface for the SecYEG complex is formed by the transmembrane span of SecE (cyan chain). The asterisk designates the proposed translocation pore in SecYEG that is plugged by the short TM2α helix. (D) An expanded top view of the L6 and L8 regions. SecE is hidden to simplify the image. The figure was created with MacPyMOL software using SEC YEG structure (PDB 1RHZ).

that basic or bulky hydrophobic residues are tolerated at this site. The top view of SecYEG shows that the side chains of four residues in L8 (R389, D390, K393, and E407) that did not cause growth defects upon mutagenesis (Fig. 7 C, yellow side chains) are closer to the membrane surface and directed away from the proposed translocation pore in the SecY subunit (Van den Berg et al., 2004). When viewed from the top, the critical residues in L6 and L8 are in three separate clusters separated by 15–20 Å (Fig. 7 D).

Point mutations in L6 and L8 of Sec61p interfere with RNC transfer to the translocation channel

How might single amino acid substitutions in L6 and L8 of Sec61p interfere with the translocation of SRP-dependent substrates? The nonadditive nature of the translocation defects displayed by the RRL6L8EE *sec61* mutant suggests that the R275E and R406E mutations affect different steps in a single pathway, not parallel pathways, leading to cotranslational translocation of SRP-dependent substrates. Attachment of an RNC complex to the translocation channel is a multistep pro-

cess that is regulated by the SRP and SR GTPases and is dependent on critical interactions between Sec61p, the ribosome, and the signal sequence (Jungnickel and Rapoport, 1995; Song et al., 2000). There are at least two steps in this reaction pathway that are likely dependent on cytoplasmic segments of the Sec61 complex. The two steps correspond to the recognition of an unoccupied translocon by a posttargeting intermediate and the docking of the ribosome onto the channel. A stable posttargeting intermediate (SR–SRP–RNC complex) is formed when SRP–RNCs are incubated with microsomes or proteoliposomes that lack a functional Sec61 complex (Song et al., 2000). The binding sites for SRP54 on the large ribosomal subunit overlap with the Sec61 binding sites, hence, SRP must dissociate from the ribosome before Sec61 attachment (Halic et al., 2004). Previously, we proposed that a direct interaction between the posttargeting intermediate and a vacant Sec61 complex facilitates the transfer of the RNC to the translocation channel after the dissociation of SRP54 from the signal sequence (Song et al., 2000). Cytosolic loops of Sec61p would be the optimal marker for an unoccupied translocon, as these segments will be occluded upon attachment of a ribosome to the translocation channel (Morgan et al., 2002). Residues in L6 of Sec61p are excellent candidates for such a recognition determinant, as point mutations in L6 (e.g., R275E) interfere with the cotranslational protein translocation pathway without causing a significant reduction in ribosome-binding affinity. Although current models for the cotranslational translocation pathway typically depict an interaction between the SR and the Sec61 complex, biochemical evidence to support this conjecture is scant.

An analysis of RNC–translocon interactions (Jungnickel and Rapoport, 1995) has indicated that the initial binding of an RNC to the Sec61 complex is sensitive to salt, and precedes signal sequence insertion into the translocation pore. Point mutations that reduce the affinity between the translocation channel and the ribosome should reduce the efficiency of RNC attachment to the translocon by destabilizing this intermediate. RNCs can bind to protease-inactivated Sec61 complexes that lack detectable affinity for nontranslating ribosomes (Raden et al., 2000), hence, signal sequence insertion into the translocation pore is not obligatorily dependent on intimate ribosome–channel contact. This may explain why certain point mutations in L8 (including R406E) do not cause a complete block in the cotranslational translocation pathway. Three-dimensional EM reconstructions of the ribosome–Sec61 complex and the RNC–Sec61 complex have revealed the presence of a 15-Å gap between the channel and the ribosome that is bridged by four stalklike connections (Beckmann et al., 2001; Morgan et al., 2002). Four connections per translocon would be consistent with the presence of three to four Sec61 heterotrimers per channel, and this would imply that a single structural element in Sec61p forms the stalklike connections. Notably, the diameter of the ribosome–channel connections observed by electron microscopy (~20 Å; Morgan et al., 2002) is very similar to the diameter of the SecY domain formed by the L6 and L8 loops (Fig. 7 D). Contact points on the ribosome for the Sec61 complex correspond to several large subunit proteins (L25, L26, and L35) and specific 25S rRNA segments (Beckmann et al., 2001; Morgan et al., 2002). Inhibition of ribosome binding to the mammalian Sec61 complex by the canine 28S rRNA, but not by the 18S rRNA, supports the conclusion that specific protein–rRNA contacts contribute to the evolutionarily conserved binding of the ribosome to Sec61p/SecY (Prinz et al., 2000a). Here, we observed that point mutations in surface exposed residues in L8 cause dramatic reductions in ribosome-binding activity, suggesting that salt bridges between the basic side chains on Sec61p and the phosphodiester backbone of the 25S rRNA are critical for ribosome attachment.

Extensive mutagenesis of *Escherichia coli* SecY has shown that R357 (R406 in Sec61p) is a crucial residue for the translocation activity of SecYEG (Mori and Ito, 2001). Suppression of the translocation defect of the *E. coli* SecY R357E mutant by "superactive alleles of SecA" has been interpreted as evidence that a functional SecA-binding site maps to the C5 region (L8) of SecY. However, other SecY point mutations (such as A363T) in L8 selectively interfere with the Ffh/FtsY-dependent integration of inner membrane proteins (Newitt and Bernstein, 1998). Clearly, this region of the translocation channel is an evolutionarily conserved segment that is critical for interaction with cytosolic effectors of the translocation pathway.

Secondary defects in posttranslational translocation

Kinetic delays in transport of the SRP-independent substrates CPY and Gas1p were observed when the *sec61* mutants were grown in rich media. Expression of Ssh1p eliminates the posttranslational transport defects caused by the *sec61* mutants, suggesting that cytosolic accumulation of SRP-dependent substrates interferes with one or more steps in the posttranslational targeting pathway. Accumulation of nontranslocated precursors in the cytosol may reduce the effective concentration of Hsp70 chaperones that deliver precursors like prepro-CPY to the Sec complex. Posttranslational translocation via the Sec complex of substrates that are normally transported by a cotranslational pathway could also cause kinetic delays in transport of posttranslational substrates by increasing precursor flux through the Sec complex.

Shared phenotypes with SRP pathway mutants

A comparison of the phenotypes of the L6 and L8 *sec61* mutants with those described for SRP-targeting pathway mutants is informative. The four to fivefold decrease in growth rate that is caused by repressing expression of SRP54 or SRα in *S. cerevisiae* (Hann and Walter, 1991; Ogg et al., 1992) is more severe than the two to threefold reductions in growth rate that are caused by point mutations in the cytosolic loops of Sec61p. The simplest interpretation of this difference is that point mutations in L6 and L8 do not eliminate the SRP-dependent targeting of RNCs to the RER, but instead interfere with the efficient transfer and attachment of the RNC to the translocation channel. The rate at which the L6 and L8 *sec61* mutants acquire a petite phenotype is less pronounced than the rapid and complete conversion of *srp54Δ* strains to a ρ^- phenotype (Hann and Walter, 1991). Although the

mechanistic link between a defect in cotranslational protein translocation and subsequent loss of mitochondrial respiration remains undefined, the morphologies of the cortical ER and the mitochondria are grossly perturbed when temperature-sensitive SRα mutants are shifted to the restrictive temperature (Prinz et al., 2000c). A third characteristic of the L6 and L8 *sec61* mutants is the transient nature of the translocation defect. Gene product depletion experiments using the GAL1/GAL10 promoter have shown that repression of SRP54 or SRα synthesis is accompanied by a severe, yet transient, defect in translocation of SRP-dependent substrates (Hann and Walter, 1991; Ogg et al., 1992). Adaptation of yeast cells to the elimination of the SRP-dependent targeting pathway occurs by induction of cytosolic chaperones and reductions in the protein synthesis rate (Mutka and Walter, 2001). The L6 and L8 *sec61* mutants described here likely adapt by a comparable mechanism.

Materials and methods

Plasmid and strain constructions

The strains used to express the *sec61* L6 and L8 mutants were derived from BWY12 (*MATα*, *trp1-1*, *ade2*, *leu2-3,112*, *ura3*, *his3-11*, *can1 sec61::HIS3*[pBW7]; provided by C. Stirling, University of Manchester, Manchester, UK). The *SSH1* gene in BWY12 was disrupted to obtain RGY400. PCR, using the plasmid pFA6a-KanMX4 as a template (Wach et al., 1994), was used to generate a DNA fragment containing a kanamycin resistance gene flanked by 5′ (nucleotides −203 to −1) and 3′ (nucleotides 1224–1470) regions from the *SSH1* gene. After transformation of BWY12, G418-resistant colonies were selected and disruption of the *SSH1* gene was confirmed by PCR. Transformation of RGY400 and BWY12 with pGAL-Kar2GFP (derived from pDN182) yielded RGY401 and RGY402, respectively. The plasmid pDN182 was provided by D. Ng (Pennsylvania State University, University Park, PA).

An NH_2-terminal His_6-FLAG tag was added to Sbh1p using a two-step PCR-based gene disruption method. The *SBH1* gene in RGY400 was disrupted using a linear DNA fragment encoding the hygromycin B resistance gene (*hph*) derived from plasmid pAG32 (Goldstein and McCusker, 1999) flanked by 5′ (−198 to −1) and 3′ (249–528) *SBH1* noncoding regions. Integration of the disruption construct into the *SBH1* locus to obtain RGY403 was confirmed by PCR analysis of hygromycin B–resistant transformants. RGY403 was transformed with a linear DNA fragment containing the following segments: (a) the 5′ noncoding region of the *SBH1* gene, (b) the Sbh1p coding sequence with a His_6-FLAG tag inserted after the initiation codon, (c) the heterologous *TRP1* gene from *Kluyveromyces lactis* (derived by PCR amplification of the plasmid pYM3; Knop et al., 1999), and (d) the 3′ *SBH1* noncoding segment. Integration of the construct into the *SBH1* locus to obtain RGY404 was confirmed by PCR analysis of trp^+ hygromycin B–sensitive transformants. Expression of epitope-tagged Sbh1p was confirmed by protein immunoblotting.

Cassette mutagenesis of Sec61

Restriction sites (PstI to SacI and XhoI to SalI) in the polylinker of pRS315 were removed by sequential rounds of double digestion, filling in with T4 DNA polymerase, followed by blunt end ligation and plasmid isolation. The resulting plasmid was designated pRS315ΔRS. Silent unique restriction sites for SalI (nt 810 relative to the ATG initiation codon), SacII (nt 825), SpeI (nt 862), and AatII (nt 901) were introduced into the coding sequence of SEC61 by PCR amplification of the plasmid pBW11 (provided by C. Stirling; Wilkinson et al., 1996), using a QuikChange mutagenesis kit (Stratagene) and synthetic oligonucleotide primers. Digestion of the resulting plasmid with HindIII yielded a 3.2-kb fragment that was cloned into the HindIII site of pRS315ΔRS to obtain the plasmid designated pZCSEC61-L6. Unique restriction sites for BamHI (nt 1111), BglII (nt 1145), XhoI (nt 1163), NcoI (nt 1196), SacI (nt 1241), and PstI (nt 1263) were introduced into plasmid pZCSEC61-L6 by the same procedure, to obtain the plasmid designated pZCSEC61-L6L8. The NcoI site in the L8 coding region causes a substitution (G399A) at a nonconserved residue in Sec61p (Fig. 2 A). The G399A mutation does not cause growth or translocation defects (not depicted).

Oligonucleotides that were 32-fold degenerate at a single codon (NNG/C on the sense strand or G/CNN on the nonsense strand) were designed to span the gap between unique restriction sites in pZCSEC61-L6 or pZCSEC61-L6L8. The oligonucleotides were annealed and ligated to double-digested ZCSEC61-L6 or pZCSEC61-L6L8 to introduce mutations in L6 or L8, respectively. *E. coli* (DH5α) was transformed with the resulting plasmid pools, and 40–60 transformants were selected for plasmid isolation and DNA sequencing.

RGY401, RGY402, and RGY404 were transformed with the pZCSEC61-L6 or pZCSEC61-L6L8 derivatives, and Leu^+ Trp^+ prototrophs were selected on SD media plates supplemented with uracil and adenine. Several transformants for each point mutant were streaked onto 5-fluoroorotic acid plates and incubated for 2 d at 30°C to select colonies that had lost pBW7. Yeast L6 and L8 *sec61* mutants were maintained on SEG media to select against ρ^- cells.

Immunoprecipitation of radiolabeled proteins and protein immunoblots

Yeast strains bearing pZCSEC61-L6 or pZCSEC61-L6L8 derivatives were transformed with the URA3-marked plasmid pDN317 (provided by D. Ng), which encodes DPAPB-HA under control of the glyceraldehyde 3-phosphate dehydrogenase promoter (Ng et al., 1996). DPAPB-HA expression is roughly 10-fold greater than that of endogenous DPAPB.

After growth at 30°C in SEG media to mid-log phase (0.2–0.6 OD at 600 nm), yeast were collected by centrifugation, resuspended in SD media, and grown for 4 h at 30°C. Yeast cells were collected by centrifugation, resuspended in fresh SD media at a density of 6 A_{600}/ml, and pulse labeled for 7 min with 100 μCi/OD Tran-^{35}S label. In pulse-chase experiments, the chase was initiated by adding unlabeled cysteine and methionine to a final concentration of 0.6 mg/ml. Radiolabeling experiments were terminated by the addition of an equal volume of 20 mM ice-cold NaN_3, followed by freezing in liquid nitrogen. Rapid lysis of cells with glass beads and immunoprecipitation of yeast proteins were performed as described previously (Rothblatt and Schekman, 1989). Spheroplasts, prepared as described below from cells grown in SD media for 4 h at 30°C, were allowed to recover for 15 min in SD media adjusted to 1.2 M sorbitol before pulse labeling. Antisera that recognize Gas1p were provided by D. Ng.

Total protein extracts were prepared as described previously (Arnold and Wittrup, 1994) from cells that had undergone 4 h of growth at 30°C in SD media. Aliquots of the protein extracts were digested with Endo H (New England Biolabs, Inc.) before CPY immunoblots. Proteins were resolved by SDS-PAGE, transferred to polyvinylidene difluoride membranes, and incubated with polyclonal or monoclonal antibodies. Antisera to Sec61p were provided by R. Schekman (University of California, Berkeley, Berkeley, CA). Peroxidase-labeled second antibodies were visualized using an ECL Western blotting detection kit (Amersham Biosciences).

Degradation of CPY^*_{HA}, expressed from the plasmid pDN431 (provided by D. Ng), was evaluated using a cycloheximide-chase protocol (Spear and Ng, 2003). Cell extracts prepared at 30-min intervals after adjustment of the culture to 100 μg/ml cycloheximide were resolved by SDS-PAGE for protein immunoblot analysis using anti-HA monoclonal antibodies. Densitometric scans of protein immunoblots were used to determine the half-life for p1 CPY^*_{HA}.

Growth curves and frequency of petite phenotype

For serial dilution experiments, yeast strains were grown in SEG media at 30°C to mid-log phase. After dilution of cells to 0.1 OD at 600 nm, 5-μl aliquots of 10-fold serial dilutions were spotted onto YPD plates that were incubated at 30° or 37°C for 2 d. RGY402 (*ssh1Δ*) did not show a colony-sectoring phenotype when grown on YPD plates, in contrast to a previous report (Wilkinson et al., 2001).

Yeast cells grown to mid-log phase in YPEG media were harvested by centrifugation and transferred to YPD media for subsequent growth at 30°C. The yeast cells were diluted into fresh media when the A_{600} reached 0.8–1 OD. After 20 generations of growth, the cells were diluted and plated onto YPD agar. After 2 d, 208 colonies were tested for respiratory competence by being replica-plated onto YPD and YPEG plates.

Cell fractionation and purification of Sec61p complexes

5 g of yeast cells grown in YPD media at 25°C to a density of 1.8 OD at 600 nm were collected by centrifugation, chilled to 4°C, adjusted to 10 mM NaN_3, and converted to spheroplasts with Zymolase (ICN Biomedicals) as described previously (Walworth and Novick, 1987). Spheroplasts were centrifuged for 10 min at 500 *g*, and broken by resuspension in 10 ml of 10 mM triethanolamine acetate, pH 7.2, 0.8 M sorbitol, and 1 mM EDTA, using a serological pipette. Microsomes were isolated from sphero-

plast lysates as described previously (Goud et al., 1988), PK-RM were prepared from yeast microsomes as described previously (Görlich and Rapoport, 1993), and spheroplast lysates from *sec61L6DDD* cells were fractionated as described previously (Gerrard et al., 2000).

Purification of the Sec61 complex was facilitated by construction of a strain (RGY404) that expresses His_6-FLAG-Sbh1p. The plasmid shuffle procedure was repeated to allow purification of the L6 and L8 *sec61* mutants from RGY404 derivatives. The Sec61 complex was purified from digitonin-solubilized PK-RM by sequential chromatography on Con-A Sepharose, Ni-NTA agarose, Q-Sepharose fast flow, and SP-Sepharose fast flow, using chromatography conditions described previously (Panzner et al., 1995) and standard chromatography methods for Ni-NTA agarose. The Sec complex was resolved from Sec61 heterotrimers by Con-A chromatography. Purification of Sec61 heterotrimers was monitored by Coomassie blue staining after SDS-PAGE and by protein immunoblot analysis using anti-FLAG and anti-Sec61p antibodies. Point mutations in Sec61p do not destabilize the Sec61p-Sbh1p-Sss1p heterotrimer. The Sec61 proteoliposomes were prepared as described previously (Song et al., 2000).

Ribosome binding to yeast PK-RM, Sec61 proteoliposomes, or Sec61 heterotrimers

Ribosomes were isolated from wild-type yeast as described previously (Beckmann et al., 1997). Loosely associated proteins were separated from 80S ribosomes by two sequential centrifugations through a high salt–sucrose cushion followed by a sucrose density gradient (10–30%) centrifugation and resuspension in 50 mM triethanolamine acetate, pH 7.5, 150 mM KOAc, and 5 mM $Mg(OAc)_2$. Binding of ^{125}I-labeled ribosomes to PK-RM or Sec61 proteoliposomes was assayed as described previously (Raden et al., 2000; Mandon et al., 2003). Membrane- or proteoliposome-bound and unbound ribosomes were separated by gel filtration chromatography (Raden et al., 2000). The cosedimentation assay to measure binding of purified Sec61p heterotrimers to ribosomes in detergent solution was performed as described previously (Prinz et al., 2000a).

We thank Colin Stirling for providing yeast strains (BWY12) and plasmids (pBW11), Davis Ng for providing plasmids (pDN182, pDN431, and PDN317) and antisera for Gas1p, and Randy Schekman for providing antisera for Sec61p.

This work was supported by National Institutes of Health grant GM35687.

Submitted: 31 August 2004
Accepted: 3 November 2004

References

Arnold, C.E., and K.D. Wittrup. 1994. The stress response to loss of signal recognition particle function in *Saccharomyces cerevisiae*. *J. Biol. Chem.* 269:30412–30418.

Baxter, B.K., P. James, T. Evans, and E.A. Craig. 1996. *SSI1* encodes a novel Hsp70 of the *Saccharomyces cerevisiae* endoplasmic reticulum. *Mol. Cell. Biol.* 16:6444–6456.

Beckmann, R., D. Bubeck, R. Grassucci, P. Penczek, A. Verschoor, G. Blobel, and J. Frank. 1997. Alignment of conduits for the nascent polypeptide chain in the ribosome-Sec61 complex. *Science.* 278:2123–2126.

Beckmann, R., C.M. Spahn, N. Eswar, J. Helmers, P.A. Penczek, A. Sali, J. Frank, and G. Blobel. 2001. Architecture of the protein-conducting channel associated with the translating 80S ribosome. *Cell.* 107:361–372.

Corsi, A.K., and R. Schekman. 1996. Mechanism of polypeptide translocation into the endoplasmic reticulum. *J. Biol. Chem.* 271:30299–30302.

Deshaies, R.J., S.L. Sanders, D.A. Feldheim, and R. Schekman. 1991. Assembly of yeast Sec proteins involved in translocation into the endoplasmic reticulum into a membrane-bound multisubunit complex. *Nature.* 349:806–808.

Finke, K., K. Plath, S. Panzer, S. Prehn, T.A. Rapoport, E. Hartmann, and T. Sommer. 1996. A second trimeric complex containing homologues of the Sec61p complex functions in protein transport across the ER membrane of *S. cerevisiae*. *EMBO J.* 15:1482–1494.

Gerrard, S.R., A.B. Mecklem, and T.H. Stevens. 2000. The yeast endosomal t-SNARE, Pep12p, functions in the absence of its transmembrane domain. *Traffic.* 1:45–55.

Goldstein, A.L., and J.H. McCusker. 1999. Three new dominant drug resistance cassettes for gene disruption in *Saccharomyces cerevisiae*. *Yeast.* 15:1541–1553.

Görlich, D., and T.A. Rapoport. 1993. Protein translocation into proteoliposomes reconstituted from purified components of the ER membrane. *Cell.* 75:615–630.

Goud, B., A. Salminen, N.C. Walworth, and P.J. Novick. 1988. A GTP-binding protein required for secretion rapidly associates with secretory vesicles and the plasma membrane in yeast. *Cell.* 53:753–768.

Halic, M., T. Becker, M.R. Pool, C.M. Spahn, R.A. Grassucci, J. Frank, and R. Beckmann. 2004. Structure of the signal recognition particle interacting with the elongation-arrested ribosome. *Nature.* 427:808–814.

Hamilton, T.G., and G.C. Flynn. 1996. Cer1p, a novel Hsp70-related protein required for posttranslational endoplasmic reticulum translocation in yeast. *J. Biol. Chem.* 271:30610–30613.

Hann, B.C., and P. Walter. 1991. The signal recognition particle in *S. cerevisiae*. *Cell.* 67:131–144.

Jungnickel, B., and T.A. Rapoport. 1995. A posttranslational signal sequence recognition event in the endoplasmic reticulum membrane. *Cell.* 82:261–270.

Knop, M., K. Siegers, G. Pereira, W. Zachariae, B. Winsor, K. Nasmyth, and E. Schiebel. 1999. Epitope tagging of yeast genes using a PCR-based strategy: more tags and improved practical routines. *Yeast.* 15:963–972.

Mandon, E.C., Y. Jiang, and R. Gilmore. 2003. Dual recognition of the ribosome and the signal recognition particle by the SRP receptor during protein targeting to the endoplasmic reticulum. *J. Cell Biol.* 162:575–585.

Morgan, D.G., J.F. Menetret, A. Neuhof, T.A. Rapoport, and C.W. Akey. 2002. Structure of the mammalian ribosome-channel complex at 17A resolution. *J. Mol. Biol.* 324:871–886.

Mori, H., and K. Ito. 2001. An essential amino acid residue in the protein translocation channel revealed by targeted random mutagenesis of SecY. *Proc. Natl. Acad. Sci. USA.* 98:5128–5133.

Mutka, S.C., and P. Walter. 2001. Multifaceted physiological response allows yeast to adapt to the loss of the signal recognition particle-dependent protein-targeting pathway. *Mol. Biol. Cell.* 12:577–588.

Newitt, J.A., and H.D. Bernstein. 1998. A mutation in the *Escherichia coli secY* gene that produces distinct effects on inner membrane protein insertion and protein export. *J. Biol. Chem.* 273:12451–12456.

Ng, D.T.W., J.D. Brown, and P. Walter. 1996. Signal sequences specify the targeting route to the endoplasmic reticulum. *J. Cell Biol.* 134:269–278.

Ogg, S.C., M.A. Poritz, and P. Walter. 1992. Signal recognition particle receptor is important for cell growth and protein secretion in *Saccharomyces cerevisiae*. *Mol. Biol. Cell.* 3:895–911.

Panzner, S., L. Dreier, E. Hartmann, S. Kostka, and T.A. Rapoport. 1995. Posttranslational protein transport in yeast reconstituted with a purified complex of Sec proteins and Kar2p. *Cell.* 81:561–570.

Pilon, M., K. Romisch, D. Quach, and R. Schekman. 1998. Sec61p serves multiple roles in secretory precursor binding and translocation into the endoplasmic reticulum membrane. *Mol. Biol. Cell.* 9:3455–3473.

Plemper, R.K., S. Bohmler, J. Bordallo, T. Sommer, and D.H. Wolf. 1997. Mutant analysis links the translocon and BiP to retrograde transport for ER degradation. *Nature.* 388:891–895.

Prinz, A., C. Behrens, T.A. Rapoport, E. Hartmann, and K.U. Kalies. 2000a. Evolutionarily conserved binding of ribosomes to the translocation channel via the large ribosomal RNA. *EMBO J.* 19:1900–1906.

Prinz, A., E. Hartmann, and K.U. Kalies. 2000b. Sec61p is the main ribosome receptor in the endoplasmic reticulum of *Saccharomyces cerevisiae*. *Biol. Chem.* 381:1025–1029.

Prinz, W.A., L. Grzyb, M. Veenhuis, J.A. Kahana, P.A. Silver, and T.A. Rapoport. 2000c. Mutants affecting the structure of the cortical endoplasmic reticulum in *Saccharomyces cerevisiae*. *J. Cell Biol.* 150:461–474.

Raden, D., W. Song, and R. Gilmore. 2000. Role of the cytoplasmic segments of Sec61α in the ribosome-binding and translocation-promoting activities of the Sec61 complex. *J. Cell Biol.* 150:53–64.

Rothblatt, J., and R. Schekman. 1989. A hitchhiker's guide to the analysis of the secretory pathway in yeast. *Methods Cell Biol.* 32:3–36.

Sommer, T., and S. Jentsch. 1993. A protein translocation defect linked to ubiquitin conjugation at the endoplasmic reticulum. *Nature.* 365:176–179.

Song, W., D. Raden, E.C. Mandon, and R. Gilmore. 2000. Role of Sec61α in the regulated transfer of the ribosome-nascent chain complex from the signal recognition particle to the translocation channel. *Cell.* 100:333–343.

Spear, E.D., and D.T. Ng. 2003. Stress tolerance of misfolded carboxypeptidase Y requires maintenance of protein trafficking and degradative pathways. *Mol. Biol. Cell.* 14:2756–2767.

Stirling, C.J., J. Rothblatt, M. Hosobuchi, R. Deshaies, and R. Schekman. 1992. Protein translocation mutants defective in the insertion of integral membrane proteins into the endoplasmic reticulum. *Mol. Biol. Cell.* 3:129–142.

Van den Berg, B., W.M. Clemons Jr., I. Collinson, Y. Modis, E. Hartmann, S.C. Harrison, and T.A. Rapoport. 2004. X-ray structure of a protein-conducting channel. *Nature.* 427:36–44.

Wach, A., A. Brachat, R. Pöhlmann, and P. Philippsen. 1994. New heterologous

modules for classical or PCR-based gene disruptions in *Saccharomyces cerevisiae. Yeast.* 10:1793–1808.

Walter, P., and A.E. Johnson. 1994. Signal sequence recognition and protein targeting to the endoplasmic reticulum membrane. *Annu. Rev. Cell Biol.* 10:87–119.

Walworth, N.C., and P.J. Novick. 1987. Purification and characterization of constitutive secretory vesicles from yeast. *J. Cell Biol.* 105:163–174.

Wiertz, E.J., D. Tortorella, M. Bogyo, J. Yu, W. Mothes, T.R. Jones, T.A. Rapoport, and H.L. Ploegh. 1996. Sec61-mediated transfer of a membrane protein from the endoplasmic reticulum to the proteasome for destruction. *Nature.* 384:432–438.

Wilkinson, B.M., A.J. Critchley, and C.J. Stirling. 1996. Determination of the transmembrane topology of yeast Sec61p; an essential component of the ER translocation complex. *J. Biol. Chem.* 271:25590–25597.

Wilkinson, B.M., J.R. Tyson, and C.J. Stirling. 2001. Ssh1p determines the translocation and dislocation capacities of the yeast endoplasmic reticulum. *Dev. Cell.* 1:401–409.

Wittke, S., M. Dunnwald, M. Albertsen, and N. Johnsson. 2002. Recognition of a subset of signal sequences by Ssh1p, a Sec61p-related protein in the membrane of endoplasmic reticulum of yeast *Saccharomyces cerevisiae. Mol. Biol. Cell.* 13:2223–2232.